Performance Evaluation Criteria for Triangular Microchannels with Smoothed Corners

Performance Evaluation Criteria for Triangular Microchannels with Smoothed Corners

Nicola Suzzi, Marco Lorenzini

Università di Udine, DPIA – Dipartimento Politecnico di Ingegneria e Architettura, Via delle Scienze 206, 33100 Udine (UD), Italy, Università di Bologna, DIN – Dipartimento di Ingegneria Industriale, Via Fontanelle 40, I-47121, Forlì (FC) Italy

marco.lorenzini@unibo.it

Abstract. The manufacturing capabilities available today for microchannels make it possible to produce in a comparatively easy, quick and cheap way several cross-sections, possibly allowing modifications of the macro-geometry. Another way is smoothing the corners of polygona cross-sections: this eliminates low-gradient areas and increases transport phenomena, i.e. frictional losses and heat transfer. Several ways of assessing the relative performance of the new shape in comparison to the original have been suggested over the years, among which are Performance Evaluation Criteria (PEC), as proposed by Bergles and Webb. PEC are based on a first-law analysis and aim at extremising the thermal power, heat exchange area, inlet temperature difference or pumping power under varying constraints. In this work equilateral triangular microchannels with uniform wall temperature are considered, through which a liquid flows in fully-developed, steady laminar regime. The cross-sectional area has its corners progressively rounded, and the velocity and temperature profiles are determined, in order to compute the Poiseuille, Nusselt and Stanton numbers, which are then employed in computing the objective functions for some PEC.

1. Introduction

Micro heat exchangers (MHXs) consist of several microchannels of various shape and surface texture which exhibit high area-to-volume ratios and high heat transfer coefficients, which makes them candidates for the removal of high specific heat fluxes, as is the case e.g. in microchips [1-3]. The capability of such microchannels to be manufactured in several shapes and their modularity provide a wide portfolio of options for enhancement of the heat transfer process, albeit at the expenses of high pressure drops, even in the higher range of the laminar regime, so much more so if the fluid is a liquid [4-6] Several strategies may be adopted for heat transfer enhancement in heat exchangers, as thoroughly discussed in [7], but promoting turbulence through inserts of various shape inside microchannels makes the modification of channel morphological characteristics a much more viable option [8-9]. This work aims at investigating the effect of changing the base cross-sectional geometry (triangular) of a microchannel by smoothing its corners. Thus, optimization of channel cross-sectional geometry is employed in this work. No viscous dissipation is considered, and Performance evaluation criteria (PEC) are used in order to determine heat transfer enhancement under defined constraints [7,10], and are sometimes coupled to second-law analyses [11]. This work complements other investigations by the same authors which dealt with other micro-geometries or boundary conditions [12-14], considered viscous dissipation [15,16] or electro-osmotic effects [17-19].

The effect of smoothing the corners of a square duct under H1 and H2 thermal boundary conditions on the Poiseuille and Nusselt numbers was investigated by [8, 9] and the numerical results used to evaluate the optimal geometrical configuration according to PECs criteria and entropy generation. In [12] the Poiseuille and Nusselt numbers was numerically computed as a function of the corners rounding radius of various cross-sectional geometry subjected to H1 boundary conditions, assuming negligible viscous heating. The effect of viscous heating on heat transfer performance was investigated, in terms of Nusselt number, in [4, 6, 15]. Here, a microchannel with a triangular cross-section and sides of equal length with rounded corners is considered. The flow is assumed Newtonian, laminar, fully developed and with negligible viscous heating. Uniform temperature is imposed at the walls.

The velocity and temperature fields are computed to obtain the Poiseuille and Nusselt numbers, which are in turn employed in the objective functions of the PEC, following the same approach as [9-13], in order to estimate the influence of the geometry of the cross-section. Results for a selection of PEC are shown and commented.

2. Statement of the problem

The geometry investigated is that of a triangular microchannels with sides of equal length, a, whose sharp corners are progressively rounded, with a radius of curvature r_c, to a limiting non-dimensional value $R_{c,max}={}^{r_c}/_{a}=1/(2\sqrt{3})$, Fig.1. Ten different values of R_c are considered. The walls of the duct have a uniform temperature T_w. The fluid flowing within the channel is incompressible, Newtonian, with thermodynamic and transport properties independent of temperature and pressure. The flow regime is pressure-driven, laminar and fully developed and viscous heating is of no significance. Forced convection is the predominant heat transfer mode and no axial conduction occurs in the fluid.

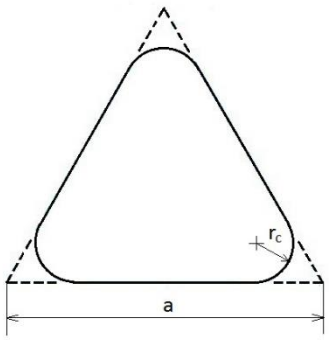

Figure 1: Triangular duct with rounded corners.

In order to compute the Poiseuille and Nusselt numbers, Po and Nu respectively, which are needed by the objective functions to be employed in the first-law optimization, the velocity and temperature fields for the fully developed flow must be determined. This is accomplished by casting the governing equations for momentum and energy conservation in non-dimensional form, Eqs. (1) and (2)

$$\frac{\partial^2 u^*}{\partial y^{*2}}+\frac{\partial^2 u^*}{\partial z^{*2}}=p^* \tag{1}$$

$$\frac{\partial^2 \vartheta^*}{\partial y^{*2}}+\frac{\partial^2 \vartheta^*}{\partial z^{*2}}=0 \tag{2}$$

Using the non-dimensional quantities defined below, Eq. (3):

$$y^*=\frac{y}{D_h},\ z^*=\frac{z}{D_h},\ u^*=\frac{u}{u_b},\ p^*=\frac{D_h^2}{\mu u_b}\frac{dp}{dx},\ \vartheta^*=\frac{T-T_w}{T_b-T_w} \tag{3}$$

Where x is the axial coordinate, y and z the coordinates related to the channel's cross-section, D_h the hydraulic diameter. The bulk velocity is u_b, whereas u is the velocity component along the channel axis, p is the pressure and μ the fluid viscosity in Pa·s. The local fluid temperature is T, whilst T_b and T_w are the bulk and wall temperatures respectively. The boundary conditions are no slip of the fluid at the wall, i.e. $u_w^*=0$ and uniform wall temperature, i.e. $\vartheta_w=0$.

The equations are then solved numerically with an approach detailed in [19]. Knowledge of u* and ϑ^* allows computation of the Nu and Po; details can be found in [13,16,19]; these quantities are then employed to compute the objective functions needed by the PEC chosen for the optimization. In general, the use of PEC allows the achievement of one of the goals listed below:

- maximise heat transfer, $\dot{Q}$;
- minimise heat transfer surface, A;
- minimise the inlet temperature difference between the bulk fluid and walls, $\Delta T_i=T_w-T_{b,i}$;
- minimise the pumping power P, which is the same as minimising the pressure drop, Δp.

The objective functions are the functional expressions for $\dot{Q}$, A, ΔT_i and P, which are dependent on six quantities, namely the shape of the channel cross-section, the channel length, L, the mass flowrate $\dot{m}$, the pumping power, P, the heat flux, $\dot{Q}$, and inlet temperature, ΔT_i.The number of channels, N, would also be an independent variable, but is not relevant for the case of a single microchannel.

Objective functions compare the value of a reference configuration to the one obtained by changing the optimisation parameter (the non-dimensional radius of curvature, in the present case) and the ratios of the two quantities are denoted by a superscript. For the heat flux the expression is

$$\dot{Q}'=\frac{\dot{Q}}{(\dot{Q})_{ref}}=\Delta T_i'\cdot\dot{m}'\ \frac{1-e^{-4\frac{Nu}{Re\,Pr}\frac{L}{D_h}}}{1-e^{-4\left(\frac{Nu}{Re\,Pr}\frac{L}{D_h}\right)_{ref}}}=\Delta T_i'\cdot\dot{m}'\ \frac{1-e^{-4\left(St\frac{L}{D_h}\right)_{ref}Nu\frac{P_h'}{\dot{m}'}\frac{L'}{D_h'}}}{1-e^{-4\left(St\frac{L}{D_h}\right)_{ref}}} \tag{4}$$

Where P_h is the heated perimeter, Re the Reynolds number, St is the Stanton number, $St=\frac{Nu}{RePr}$. For the pumping power, the objective function, where A_c is the cross-sectional area, is

$$P'=\frac{P}{(P)_{ref}}=\frac{(f\,Re)'\ \dot{m}'^2\ L'}{A_c'\ D_h'^2} \tag{5}$$

2.1. Geometrical constraints

The reference configuration corresponds to a cross-section with sharp corners (R_c=0). It is easily seen that the expression for D_h, A_c,and P_h, all depend on both the non-dimensional radius of curvature and the length of the cross-section side, a'. This behaviour is not shared by the Poiseuille and Nusselt numbers, which are independent of the length a. If the objective functions are to be optimised with respect to R_c, four different cases must be treated, each with a different geometrical constraint which eliminates any dependence on the length a, see Table 1.

Geometric constraint	a/a_{ref} ratio
$\frac{a}{a_{ref}}=1$	$\frac{a}{a_{ref}}=1$

$D_h'=1$	$\frac{a}{a_{ref}}=\frac{1}{2\sqrt{3}}\frac{\left(3+2R_c\left(\pi-3\sqrt{3}\right)\right)}{\left(\frac{\sqrt{3}}{2}+R_c^2\left(\pi-3\sqrt{3}\right)\right)}$
$P_h'=1$	$\frac{a}{a_{ref}}=\frac{1}{\left(1+R_c^2\,\frac{2}{3}\left(\pi-3\sqrt{3}\right)\right)}$
$A_c'=1$	$\frac{a}{a_{ref}}=\sqrt{\frac{1}{\left(1+R_c^2\,\frac{2}{\sqrt{3}}\left(\pi-3\sqrt{3}\right)\right)}}$

Table 1 – Constrained geometrical parameters (left) and corresponding expression of a' (right).

For each PEC the choice of the geometrical constraint determines one expression of the objective function.

In the following section, some examples of PECs are given, after showing examples of velocity and temperature fields and the Poiseuille and Nusselt numbers as a function of the radius of curvature.

3. Results and discussion

Figure 2a shows the velocity distribution over the cross-section in the case of sharp corners, whilst Fig. 2b shows the same quantity when the corners are smoothed at half the maximum allowable radius of curvature.

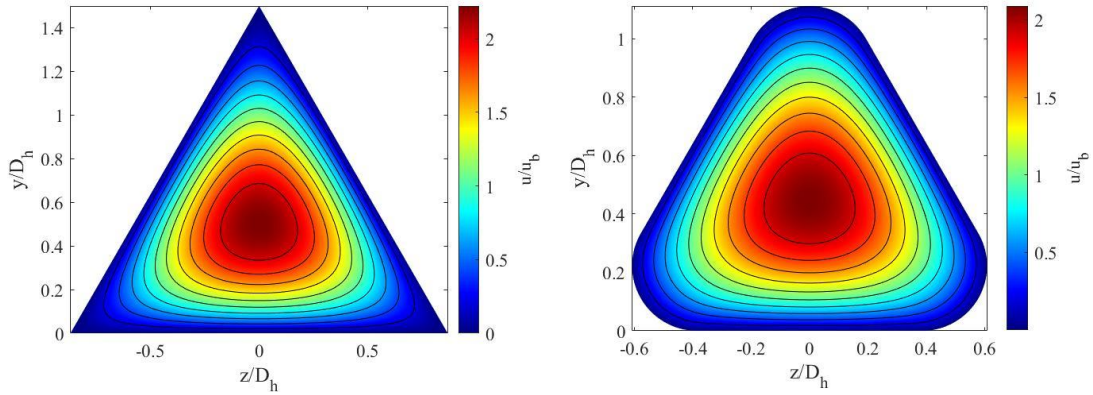

Figure 2: Velocity profile for R_c=0 (a) and R_c=$R_{c,max}$/2 (b).

The maximum velocity is in the barycentric position in both cases, but when R_c=0 the value is higher. This is due to fluid stagnation at the sharp corners, which does not occur when they are smoothed; this implies that local gradients are larger in the latter case, as confirmed by the temperature distribution, Fig. 3. The larger gradients at the smoothed corners of the cross-section signal an increase in transport phenomena, which is captured by the trends of the Poiseuille and Nusselt numbers, plotted in Fig. 4. It

should be noted that the maximum increase in Po is below 20%, and that the Poiseuille number remains almost constant for R_c>0.15, whereas the Nusselt number increases monotonically with R_c up to about 45% more than the value it attains for the base cross-section. It should also be pointed out that the local value of the Nusselt number along the heated perimeter varies sharply, with maxima at the midpoint of each side and minima at the corners, but for sharp corners the minima are close to zero and increase steadily with R_c; the maxima, conversely, increase at first, reaching a maximum at around half $R_{c,max,}$.

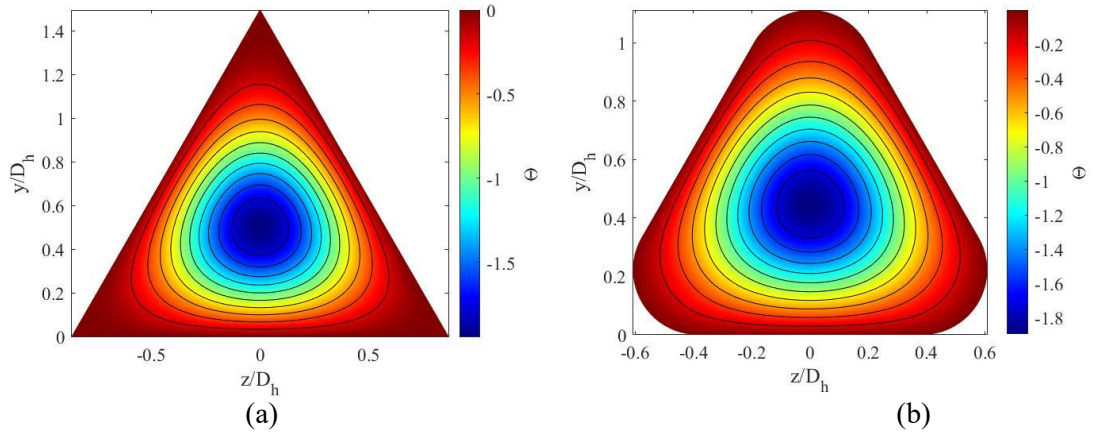

Figure 3: Temperature profile for R_c=0 (a) and R_c=$R_{c,max}$/2 (b).

For larger radii, the straight portion of the sides shortens and the maximum Nusselt drops below the value for R_c=0, but the average value increases, hence the trend of Fig. 4b.

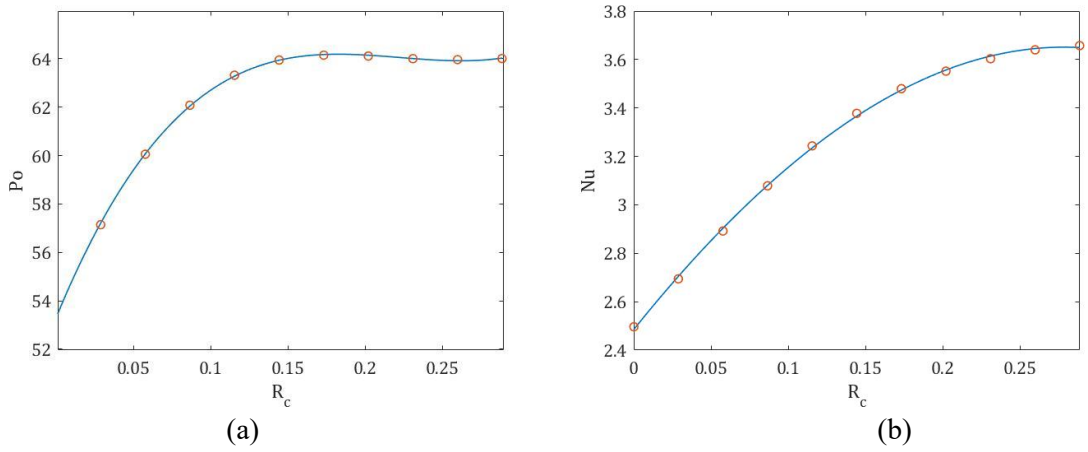

Figure 4: Poiseuille number (a) and Nusselt number (b) as a function of R_c.

3.1. PEC optimisation

Once the Poiseuille and Nusselt numbers are determined, PEC optimization can be carried out using algebraic expressions such as, Eqs.(4) and (5) [13], some cases are presented below. If most quantities are normalized using the corresponding values for the base geometry (R_c=0), some reference values had to be assumed for the Reynolds number (Re_{ref}=5), the Prandtl number (Pr=7 throughout), the channel length (L=5 mm) and its hydraulic diameter ($D_{h,ref}$=100 μm). Since the two objective

functions depend on five different quantities, three of them must be kept constant in turn. The triplet of variables which do not change as R_c is varied determines the kind of PEC which is applied.

3.1.1. FG2a. Maximisation of the heat transfer (so-called FG1a PEC) under fixed inlet temperature difference, length and mass flowrate and minimisation of ΔT_i if $\dot{Q}$, L and $\dot{m}$ are kept constant (called FG1b PEC) show that the radius of curvature has no practical influence and is therefore neglected here. The PEC FG2a involves maximisation of the heat transfer with ΔT_i, L and P constant. After some calculations it can be demonstrated that Eq.(4) becomes

$$\dot{Q}'=C_1\left(\frac{a}{a_{ref}}\right)^2\frac{1-e^{-\frac{C_2}{\left(\frac{a}{a_{ref}}\right)^2}}}{C_3} \tag{6}$$

Where C_1, C_2 C_3 are functions of the radius of curvature only, and therefore independent of a/a_{ref}. Because of this, the value of $\dot{Q}'$ is dependent on the geometrical constraint chosen from those in Table 1. This is clearly shown in the four plots of Fig. 5a, which represent the different trends of the heat flux as the radius of curvature is varied: when the side length is kept constant, the increase is moderate at best, with a maximum around 9% at $R_c\cong0.25$. For all other cases the trend is monotonous and has its extreme value (a minimum for D_h= constant, a maximum in the two remaining instances) for the highest radius of curvature; it should be remarked that the cross section becomes circular then.

3.1.2. FG2b. The mirror case to FG2a is FG2b, where the minimum inlet temperature difference is sought for fixed heat flux, channel length and pumping power. Again, after some algebraic manipulations, Eq.(4) can be cast into the form of Eq. (7):

$$\Delta T_i'=\frac{1}{C_1\left(\frac{a}{a_{ref}}\right)^2}\frac{C_3}{1-e^{-\frac{C_2}{\left(\frac{a}{a_{ref}}\right)^2}}}=\dot{Q}'^{-1} \tag{7}$$

As is to be expected, the trends shown in Fig. 5b are the reverse of the previous criterion, and the configuration yielding the best results (for maximum radius of curvature) is the one with constant heated perimeter. In this case the reduction is dramatic, with ΔT_i dropping to 50% of the reference value for $R_c\cong0.2$ and decreasing further to 35% of the original for the maximum radius of curvature.

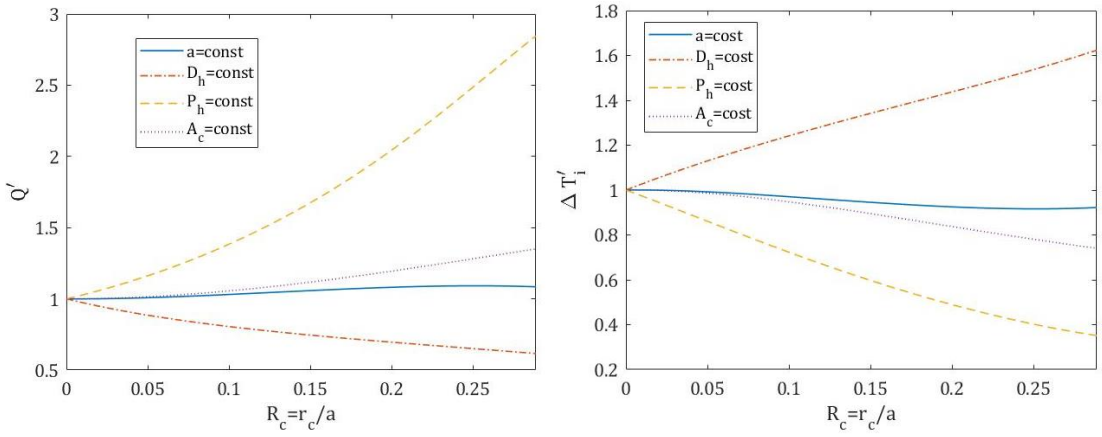

(a) (b)

Figure 5 – Local heat transfer coefficient along the heated perimeter (a) and temperature profile (b) on the mid-plane.

3.1.3. FN1. The FN-type criteria have minimisation of either the channel's length or the pumping power as their goals. The FN1 criterion has the heat transfer, inlet temperature difference and pumping power as constraints, i.e. quantities that are held fixed throughout the optimisation and L as its objective function. Contrary to the previous cases, this leads to an expression which is not explicit in L', as shown in Eq. (8):

$$L' = \left[C_1 \left(\frac{a}{a_{ref}} \right)^2 \frac{1-e^{-C\frac{C_2}{\left(\frac{a}{a_{ref}}\right)^2}(L')^{\frac{3}{2}}}}{C_3} \right]^2 \tag{8}$$

In this case, care must be exerted to limit the non-dimensional quantities to physically significant values, lest the results become negative, therefore meaningless. This was considered when choosing the reference values mentioned in the opening paragraph of this section.

Equations (6) and (8) only differ for $(L')^{\frac{3}{2}}$ in the exponential term; unsurprisingly, that the trend of L' is similar to that of $\dot{Q}$, as, results from the comparison of Figs. 5a and 6a. It is therefore concluded that only when the hydraulic diameter is fixed does smoothing the corner bring a benefit, and that this shortening of the channels is larger, the more the cross-section approaches the circular channel. Among the remaining constraints, geometries with fixed side exhibit little sensitivity to the radius of curvature, whilst a fixed heated perimeter causes a stronger increase in the channel's length the higher the value of R_c.

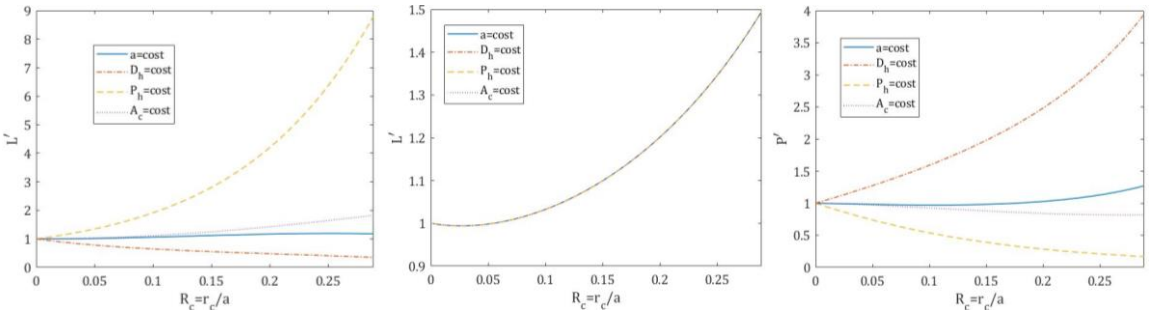

(a) (b) (c)

Figure 6 Change in channel length for the FN criteria: FN1 (a), FN2 (b) and FN3 (c).

3.1.4. FN2. Another criterion to minimize the channel's length is known as FN2; in this case the constraints are fixed heat flux, inlet temperature difference and mass flowrate, $\dot{Q}', \Delta T_{in}', \dot{m}' = 1$. When theys are applied, the objective function becomes Eq. (9):

$$L' = \frac{D_h'}{P_h'} \frac{1}{Nu'} \tag{9}$$

Since both D_h' and P_h' are proportional to the a/a_{ref} ratio, L' is a function of Nu', which is dependent on R_c only: as a consequence, the four curves for the geometrical constraint all collapse onto one, as shown in Fig. 6b, which demonstrates how L' grows with the radius of curvature for R_c>0.1 and is insensitive to it for values below this threshold.

3.1.5. FN3. The criterion FN3 strives to minimize the pumping power, P', under the same constraints as FN2, i.e. fixed heat flux, inlet temperature and mass flowrate. Again, the objective function can be recast accounting for the constraints, into the form provided by Eq. (10)

$$P' = C_1 \left(\frac{a}{a_{ref}} \right)^{-4} \tag{10}$$

Where C_1 is a constant which depends on R_c only. The corresponding trend for the four geometrical constraints is shown in Fig. 6c and are essentially monotonous with the radius of curvature, with a sharp increase in the case of a fixed hydraulic diameter and a strong decrease in the case of fixed heated perimeter, the remaining cases having much smaller changes, with an increase in pumping power for fixed side and a decrease for fixed cross-sectional area.

4. Conclusions

In this work, the Poiseuille and Nusselt numbers for the fully-developed, laminar flow of a Newtonian fluid through a triangular microchannel with smoothed corners and uniform wall temperature have been computed, and the results used in the PECs for microchannel optimisation, using the heat flux and the pumping power as the objective functions. It has been demonstrated that smoothing the corners enhances the transport phenomena, which result in augmented momentum transport (hence Po goes from around 53 to 64 when $R_c \cong 0.10$ and remains almost constant thereafter) and heat transfer (with Nu increasing from around 2.5 to 3.64 at $R_c \cong 0.26$). The values of Po and Nu have then been used to analyse different PECs. It has been demonstrated that one further geometrical constraint must be applied in most cases if the objective functions (enhanced heat flux and pumping power) are to be optimised as a function of the radius of curvature only. For several criteria the results have been presented quantitatively and commented. It is hoped that the paper can contribute some general indications at design level and help comprehension of the transport phenomena in triangular microchannels.

References

[1] Ohadi M, Choo K, Dessiatoun S and Cetegen E E, *2013 Next Generation Microchannel Heat Exchangers*; (Springer New York, NY USA; Berlin/Heidelberg)
[2] Lorenzini M, Fabbri G and Salvigni S. *2007 Appl. Therm. Eng.* **27**(5-6) pp 969-975
[3] Kew P and Reay D, *2011 Appl. Therm. Eng.* **31**(5) pp 594-601
[4] Yang Y, Chalabi H, Lorenzini M, and Morini G L, *2014 Heat Tr. Eng.* **35**(2), pp 159–170
[5] Morini G, Lorenzini M, Colin S, and Geoffroy S, *2006 Proc. of ICNMM2006*, **A,** (ASME, New York, NY) pp. 411–418.
[6] Morini G L, Yang Y and Lorenzini M, *2012 Experimental Heat Transfer* **25**(3), pp 151–171
[7] Webb R L, *1994 Principles of Enhanced Heat Transfer*, (Wiley, New York)
[8] Ray S and Misra D, *2010 Int. J. of Th. Sci.* **49**, pp 1763–1775
[9] Chakraborty S. and Ray S, *2011 Int. J. of Th. Sci.* **50**, pp 2522–2535
[10] Saha S K, Ranjan H, Emani S M and Barthi A K, *2020 Performance Evaluation Criteria in Heat Transfer Enhancement* (Springer New York, NY USA; Berlin/Heidelberg)
[11] Petkov V M and Zimparov V D, *2013 Int.l Review of Chem. Engineering* **5**, pp 74–87
[12] Lorenzini M and Morini, *2011 Heat Transfer Engineering* **32(13-14)**, pp 1108–1116
[13] Lorenzini M and Suzzi N, *2016 Heat Transfer Engineering* **37** (13-14), pp 1096–1104
[14] Lorenzini M, Daprà I, and Scarpi G, *2017 Applied Thermal Engineering* **122**, pp 118–125
[15] Lorenzini M, *2013 Houille Blanche* **4**, pp 64–71
[16] Suzzi N and Lorenzini M, *2019 Int. J. of Th. Sci.,* **145** 106032
[17] Morini G L, Lorenzini M, Salvigni S, and Spiga M, *2006 Int. J. of Th. Sci.* **45**(10), pp 955–961
[18] Lorenzini M, *2020 Thermal Science Engineering Progress* **19** 100617
[19] Suzzi N and Lorenzini M *2021 Fluids* **1,** 1010000